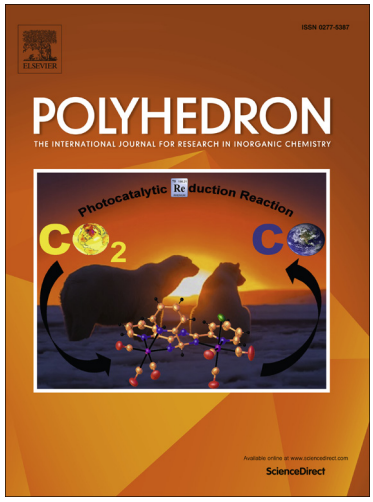

Supramolecular Nickel Complex Based on Thiosemicarbazone. Synthesis, Transfer hydrogenation and Unexpected Thermal behavior

Şükriye Güveli, Tülay Bal-Demirci, Bahri Ülküseven, Namık Özdemir

PII: S0277-5387(16)00084-X
DOI: http://dx.doi.org/10.1016/j.poly.2016.02.002
Reference: POLY 11814

To appear in: *Polyhedron*

Received Date: 30 September 2015
Accepted Date: 3 February 2016

Please cite this article as: Ş. Güveli, T. Bal-Demirci, B. Ülküseven, N. Özdemir, Supramolecular Nickel Complex Based on Thiosemicarbazone. Synthesis, Transfer hydrogenation and Unexpected Thermal behavior, *Polyhedron* (2016), doi: http://dx.doi.org/10.1016/j.poly.2016.02.002

Supramolecular Nickel Complex Based on Thiosemicarbazone. Synthesis, Transfer hydrogenation and Unexpected Thermal behavior

Şükriye Güveli[a], Tülay Bal-Demirci,[a,*] Bahri Ülküseven[a] and Namık Özdemir[b,*]

[a] Department of Chemistry, Engineering Faculty, Istanbul University, 34320, Istanbul, Turkey

[b] Department of Physics, Faculty of Arts and Sciences, Ondokuz Mayıs University, 55139, Samsun, Turkey

ABSTRACT: The cationic thiosemicarbazone complex of nickel containing triphenylphosphine as coligand was synthesized through the isopropanol-assisted hydrogen transfer reaction. The thiosemicarbazone ligand (LH_2) and its cationic nickel complex, $[Ni(LH)(PPh_3)]^+Cl^-.(CH_3)_2CHOH$, were characterized by elemental analysis, IR, ^{1}H-NMR and UV-Vis. spectroscopies. The molecular structure of the complex was also determined by single crystal X-ray diffraction technique. In addition computational studies at B3LYP/6–311G(d,p) (main group) and LANL2DZ (Ni) level were carried out for theoretical characterization of the ligand and complex. Structural analysis of the complex indicated the presence of square-planar coordination geometry (ONNP) about nickel in which the thiosemicarbazone ligand coordinated as mononegative tridentate. Isopropyl alcohol catalyzed efficiently the transfer hydrogenation and the cationic complex formed through inter conversion azinyl-azinylidene. All spectral data support the formation of the ligand and its nickel complex and the results calculated using theoretical methods coincide well with the experimental findings. The thermal degradation of the complex was investigated using thermogravimetric and differential thermal analyses techniques in nitrogen and oxygen atmosphere. The oxidative-thermal decomposition of the compound showed volatilization of nickel as unexpected behavior unlike nitrogen atmosphere.

Keywords: Thiosemicarbazone, Transfer hydrogenation, Nickel, X-Ray diffraction, Isopropyl alcohol.

1. Introduction

Thiosemicarbazones are of great importance because of biological, medicinal, pharmacological and analytical properties[1-11]. They have more than one binding site for metal ions and their properties change depending on metal atom, coordination modes, connected aldehyde or ketone and substituents on aldehyde/ketone[12-16].

Thiosemicarbazones possess different coordination modes, can be in neutral or anionic form because of thione-thiol tautomerism and give generally neutral or rarely cationic metal complexes (Scheme 1) [17-25].

Scheme 1. Tautomerism of Thiosemicarbazone

Supramolecular structures have attracted great attention in recent years and take place as a result of an intermolecular hydrogen bonding, pi-pi interactions, electrostatic effects, hydrophobic forces, metal coordination and van der Waals forces[26]. The noncovalent interactions are extremely significant in catalysis. Although there are a great number of papers on thiosemicarbazones owning more than one donor atom, the papers are limited on supramolecular structures of metal complexes based on thiosemicarbazone[27-29].

As a continuation of our interest on thiosemicarbazone and its metal complexes, we present here the synthesis, structural, thermogravimetric and spectroscopic features of 5-bromo-2-hydroxy-benzaldeyde-S-methly-isothiosemicarbazido triphenylphosphine nickel chloride isopropyl alcohol. In this study, we isolated rarely occurring nickel complex salt form of S-methyl isothiosemicarbazone and triphenylphosphine, also containing one mole isopropyl alcohol as solvent in formula $[Ni(LH)(PPh_3)]^+Cl^-.(CH_3)_2CHOH$. Moreover, this solute-solvent complex has supramolecular structure (**I**). Despite many attempts in previous study, we were unable to put solvent molecule in the same crystal lattice as stable complex and the crystal did not contain chloride anion and the complex was in neutral form, $[NiLPPh_3]$, (Scheme 2)[30]. By this study, we not only obtained rarely occurring cationic complex salt (**I**) by changing polarity of solvent, but we also saw that the isopropyl alcohol catalyzed efficiently the transfer hydrogenation and caused to supramolecular structure's formation.

Moreover, thermal decomposition of this crystal (**I**) showed an unexpected behavior in oxygen and nitrogen atmosphere. The oxidative decomposition of the complex unlike nitrogen atmosphere displayed volatilization of nickel. This property is preferable for volatile solid metallo-organic precursors for use in CVD applications for preparing thin films of metallic nickel[31,32].

Corresponding Authors : Tulay Bal-Demirci, E-mail: tulaybal@istanbul.edu.tr, tel. +902124737070-17677, fax. +902124737180,
Namık Özdemir, E-mail: namiko@omu.edu.tr, tel. +903623121919-5256, fax. +903624576081

Scheme 2. Formation of [NiLPPh$_3$] and [Ni(LH)(PPh$_3$)]$^+$Cl$^-$.(CH$_3$)$_2$CHOH **(I)**

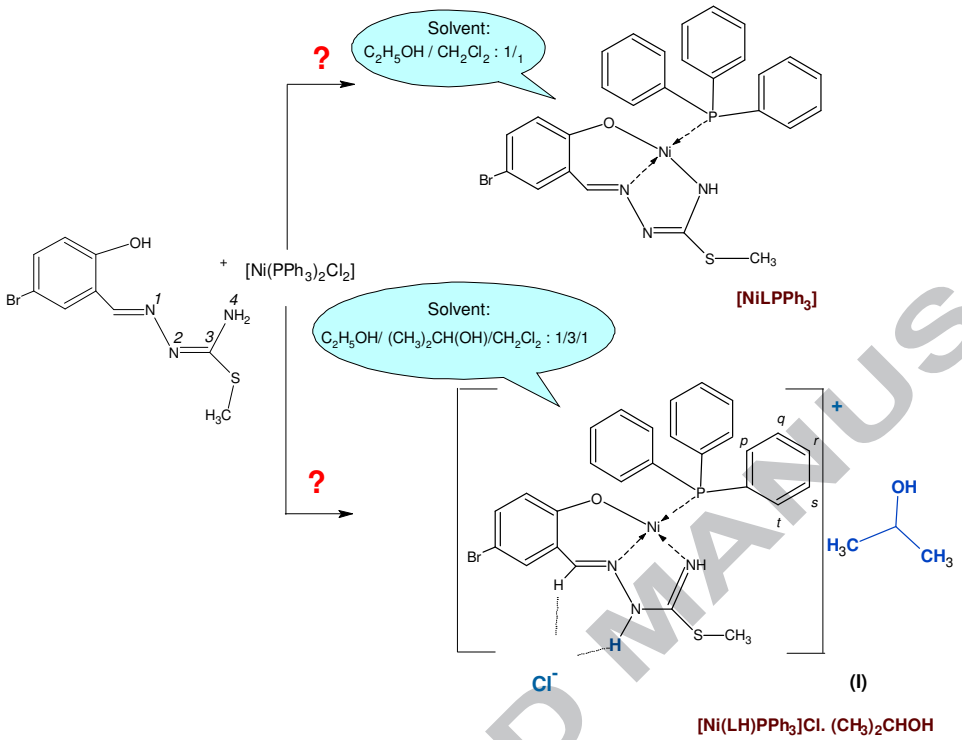

2. Experimental

2.1. General Remarks

All chemicals were of reagent grad and used as commercially purchased without further purification. The elemental analyses were determined on a Thermo Finnigan Flash EA 1112 Series Elemantar Analyser and Varian Spectra–220/FS Atomic Absorption spectrometer. IR spectra of the compounds were recorded on KBr pellets with a Mattson 1000 FT-infrared spectrometer. The ^{1}H-Nuclear Magnetic Resonance spectra were recorded in DMSO on Bruker AVANCE-500 model spectrometer. UV–Vis spectra were obtained with a Shimadzu 2600 UV–Visible Spectrometer as 5 x 10^{-5} M solutions in $CHCl_3$. Magnetic measurements were carried out at room temperature by the Gouy technique with an MK I model device obtained from Sherwood Scientific. The molar conductivities of the compounds were measured in 10^{-3} M DMSO solution at 25±1°C using a digital WPA CMD 750 conductivity meter. Thermal study of complex was carried out on a Seiko Exstar 6000 TG/DTA 6300 instrument between the 0 and 1000 °C at a heating rate of 5 °C/ min. under air and nitrogen atmosphere using platinum crucibles.

2.1.1.Synthesis of 5-Bromo-2-hydroxy-benzaldeyde-S-methly-isothiosemicarbazone (LH$_2$). The ligand was prepared according to common procedures[30]. The color; m.p. (°C); yield (%); elemental analysis; UV-Vis. [λ_{max}(ε): nm (mM^{-1}cm^{-1}); IR (cm^{-1}) and ^{1}H-NMR (ppm, *J* in Hz) data of the ligand were given as follows: Yellow; 199; 91; *Anal*. Calc. for $C_9H_{10}BrN_3OS$ (288.16 g/mol): C 37.51, H 3.50, N 14.58, S 11.13, Found: C 37.53, H 3.49, N 14.57, S 11.11%; UV-Vis.: 241 (4.05), 298 (5.12), 309 (4.06), 342 (4.06), 356 (4.01); IR: ν_a(NH$_2$) 3476; ν_s(NH$_2$) 3276; ν(OH) 3084; δ(NH$_2$) 1632; ν(C=N^1) 1620; ν(C=N^2) 1607; ν(C-O) 1153; ^{1}H-NMR: 11.65, 10.79 (cis/trans ratio: 3/2, s, 1H, O*H*), 8.43, 8.33 (syn/anti ratio:2/3, s, 1H, C*H*=N^1), 7.01 (s, 2H, N^4*H*$_2$), 7.76 (d-d, *J*=2.52, 1H, *c*), 7.35 (m, 1H, *b*), 6.86 (d-d, *J*=1.52, *J*=8.7, 1H, *a*), 2.45, 2.39 (cis/trans ratio:3/2, s, 3H, S-C*H*$_3$).

2.1.2. Synthesis of [Ni(LH)(PPh$_3$)]$^+$Cl$^-$(CH$_3$)$_2$CHOH. The compound (**I**) was prepared with small modifications of literature method (Scheme 2)[33]. [Ni(PPh$_3$)$_2$Cl$_2$](0.65 g, 1 mmol) in 25 mL absolute alcohol was added to the solution of LH$_2$ (0.29 g, 1 mmol) in mixture of ethanol, isopropyl alcohol and dichloromethane (20 ml: 60 mL: 20mL). The reaction mixture was refluxed for 48 h. After standing for six days, the precipitated dark red crystals were filtered off and washed with *n*-hexan (10 ml). The color; m.p. (°C); yield (%); $\mu_{eff.}$ value (BM); molar conductivity (ohm^{-1}cm^{2}mol^{-1}); elemental analysis; UV-Vis. [λ_{max}(ε): nm (mM^{-1}cm^{-1})]; IR (cm^{-1}) and ^{1}H-NMR (ppm, *J* in Hz, *p-t* are the symbols for the PPh$_3$ protons) data of the nickel complex were given as follows: Red; 177-178; 63; 0.12; 32; *Anal*. Calc. for $C_{30}H_{32}BrClN_3NiO_2PS$ (703.68 g/mol): C 51.21, H 4.58, N 5.97, S 4.56, Found: C 51.38, H 4.41, N 6.09, S 4.62%; UV-Vis.: 239 (4.13), 263 (4.12), 355 (3.53), 386 (3.49), 406 (3.55) 529 (2.66); IR: ν(NH) 3265, 3123, δ(NH) 1630, ν(C=N) 1562, 1520, ν(C-S) 750, ν(PPh$_3$) 1435, 1100, 696, isopropyl ν(C-H) 2965, 2920, 2814; ^{1}H-NMR: 11.61, 10.75 (N^{2}H, 1H), 8.41, 8.30 (CH=N, 1H), 7.61 (s, 1H, c), 7.39 (brd

s, 9H, *p*, *t*, *r*), 7.91, 6.99 (brd N^4H, 1H), 7.35 (dd, *J*=2.44, *J*= 8.78, 1H, *b*), 7.22 (brd s, 6H, *q*, *s*), 6.83 (d, *J*= 8.79, 1H, a), 2.41 (s, 3H, S-CH_3), isopropyl alcohol: 4.30 ppm (s, 1H, OH), 3.75 (m, 1H, -CH), 1.02 (d, *J*=5.86, 6H, -CH_3).

2.2. X-ray analysis. Intensity data of the compound (**I**) were collected on a STOE IPDS II diffractometer at room temperature (296 K) using graphite-monochromated Mo Kα radiation (λ=0.71073 Å) by applying the ω-scan method. Data collection and cell refinement were carried out using X-AREA[34] while data reduction was applied using X-RED32[34].The structure was solved by direct methods using SHELXS-2013[35] and refined with full-matrix least-squares calculations on F^2 using SHELXL-2014[35]implemented in WinGX[36] program suit. All H atoms were inserted in idealized positions and treated using a riding model, fixing the bond lengths at 0.82, 0.86, 0.93, 0.98 and 0.96 Å for OH, NH, aromatic CH, methine CH and CH_3 atoms, respectively. The displacement parameters of the H atoms were fixed at $U_{iso}(H) = 1.2U_{eq}$ ($1.5U_{eq}$ for OH and CH_3) of their parent atoms.

2.3. Computational details. The ligand and title compound were optimized using the spin-restricted hybrid DFT (B3LYP) method[37, 38].In the optimization process, nickel has been represented by the widely used quasi-relativistic LANL2DZ basis set (Los Alamos effective core pseudo-potential plus double-ζ)[39-41], while 6−311G(d,p) basis set[42,43] has been assigned to the remaining atoms. The ^{1}H-NMR chemical shifts were calculated within the gauge-independent atomic orbital (GIAO) approach[44,45] applying the same method and the basis sets as used for geometry optimization. All the calculations were performed by using Gauss View molecular visualization program[46] and Gaussian 03W program package[47]. The effect of solvent on the theoretical NMR parameters was included using the default model IEF-PCM (Integral-Equation-Formalism Polarizable Continuum Model)[48] provided by Gaussian 03W. Dimethylsulfoxide with a dielectric constant (ε) of 46.7 was used as solvent. Chloroform with a dielectric constant (ε) of 4.90 was used as solvent. All the geometry optimizations were followed by frequency calculations and no imaginary frequencies were found, approving the stable nature of the optimized structures. A scaling factor of 0.9811 was used to correlate the calculated vibrational frequencies with the experimental ones. The electronic absorption spectra were calculated using the time-dependent density functional theory (TD-DFT) method[49,50].

3. Results and Discussion

In this study, we have synthesized a new supramolecular complex structure (**I**) from the reaction of 5-bromo-2-hydroxy-benzaldeyde-S-methly-isothiosemicarbazone with triphenylphosphine in the presence of nickel(II) in a proper solvent mixture. The ligand and nickel complex are soluble in common organic solvents such as CH_2Cl_2, $CHCl_3$, EtOH, DMSO, ethyl acetate, etc. The ligand and complex were characterized by a combination of FT-IR, ^{1}H-NMR, UV-Vis. and elemental analysis. Theoretical characterization of the ligand and complex was achieved using the density functional theory (DFT) method.

Interesting results were obtained from thermal analysis (TGA and DTA) of the formed complex. The structure of the complex was obtained by single-crystal X-ray diffraction technique. By this study, we not only obtained rarely occurring cationic complex salt (**I**) by changing polarity of solvent, but we also saw that the isopropyl alcohol catalyzed efficiently the transfer hydrogenation and caused to tautomeric interconversion azinyl-azinylidene type and to supramolecular structure.

3.1. Experimental and theoretical structure. To confirm the exact structure of the complex, X-ray crystallographic analysis has been carried out. The details of the data collection and structure solution are collected in Table 1. ORTEP-3[36] diagram of the complex is shown in Fig. 1, while the important bond lengths and angles are given in Table 2. The complex crystallizes in the triclinic space group $P\bar{1}$ with an isopropyl alcohol molecule in the asymmetric unit.

Table 1.

Crystal Data and Structure Refinement Parameters for the Title Compound

CCDC deposition no.	1044168
Color/shape	Brown/prism
Chemical formula	$[Ni(C_9H_9BrN_3OS)(C_{18}H_{15}P)]^+ \cdot Cl^- \cdot C_3H_8O$
Formula weight	703.68
Temperature (K)	296
Wavelength (Å)	0.71073 Mo Kα
Crystal system	Triclinic
Space group	$P\bar{1}$ (No. 2)
Unit cell parameters	
a, *b*, *c* (Å)	8.9868(6), 10.9945(7), 17.2003(12)
α, β, γ (°)	71.220(5), 76.089(5), 84.943(5)
Volume (Å^3)	1561.71(19)
Z	2
D_{calc} (g/cm^3)	1.496
μ (mm^{-1})	2.136
Absorption correction	Integration
T_{min}, T_{max}	0.5115, 0.8284
F_{000}	720
Crystal size (mm^3)	0.62 × 0.28 × 0.09
Diffractometer	STOE IPDS II
Measurement method	ω scan
Index ranges	$-11 \le h \le 11$, $-14 \le k \le 14$, $-22 \le l \le 22$
θ range for data collection (°)	$1.957 \le \theta \le 27.590$
Reflections collected	28874

Independent/observed reflections	7198/5297
R_{int}	0.0508
Refinement method	Full-matrix least-squares on F^2
Data/restraints/parameters	7198/0/361
Goodness-of-fit on F^2	1.041
Final R indices [$I > 2\sigma(I)$]	$R_1 = 0.0403$, $wR_2 = 0.0908$
R indices (all data)	$R_1 = 0.0619$, $wR_2 = 0.0977$
ρ_{max}, $\Delta\rho_{min}$ (e/Å^3)	0.41, −0.50

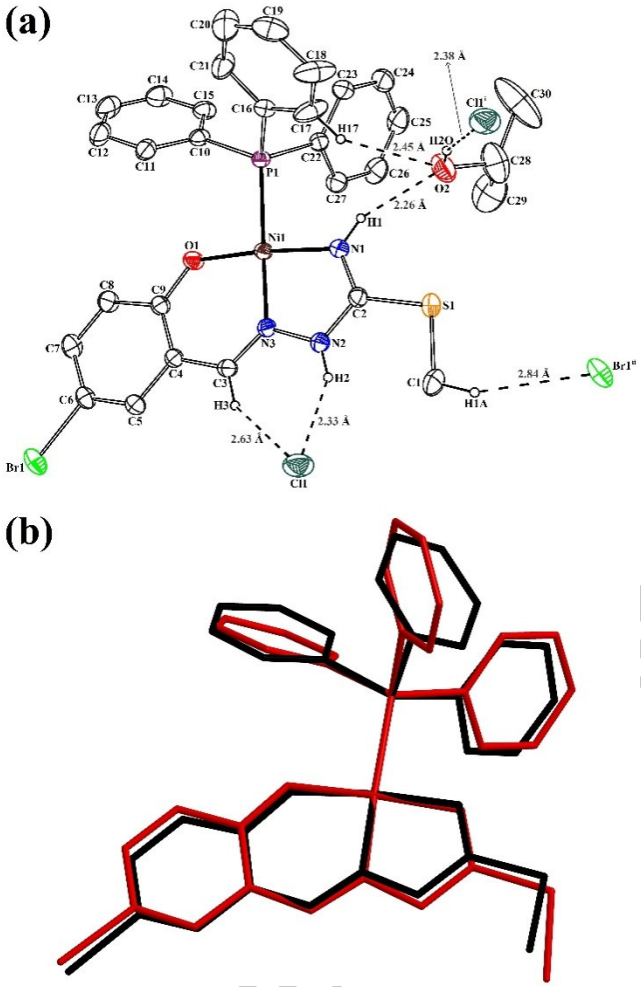

Fig. 1. (a)A view of the title complex showing 20% probability displacement ellipsoids and the atom-numbering scheme. For clarity, only H atoms involved in hydrogen bonding (dashed lines)have been included. [Symmetry codes: [i] $-x + 1, -y + 1, -z + 1$; [ii] $x + 1, y - 1, z$.] (b) Atom-by-atom superimposition of the structures calculated (red) over the X-ray structure (black) for the cationic complex. Hydrogen atoms are omitted for clarity.

In the complex, the thiosemicarbazone ligand is coordinated to nickel by using its phenolic oxygen, azomethine nitrogen and isothioamide nitrogen atoms and behaved as a monobasic O,N,N tridentate donor by forming five- and a six-membered chelate rings with N—Ni—N and O—Ni—N bite angles of 82.44(9)° and 93.46(8)°, respectively. A phosphorus atom of the triphenylphosphine ligand satisfies the fourth coordination site in the complex. In the molecule, the charge of the cationic complex is neutralized by a Cl^- anion.

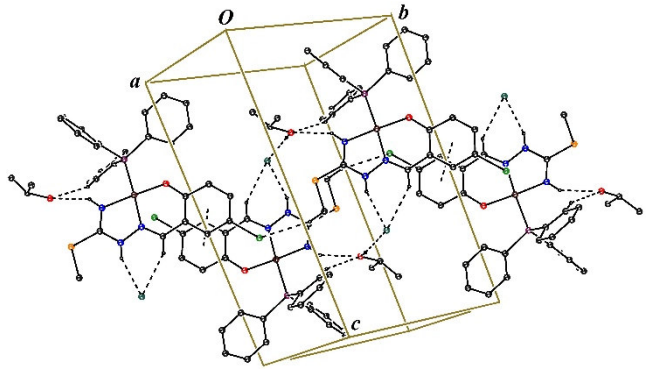

Fig. 2. Part of the crystal structure of the title complex. Broken lines show the intermolecular interactions. For clarity, H atoms not involved in H-bonds have been omitted.

In the square-planar coordination, atoms Ni1, P1, O1, N1 and N3 deviate by −0.0116(8), 0.0724(9), −0.0748(11), −0.0788(11) and 0.0928(11) Å, respectively, from the mean plane through these five atoms. The thiosemicarbazone ligand is planar with an r.m.s. deviation of the non-H atoms being 0.0239 Å, and makes a dihedral angle of 4.704(8)° with the coordination plane. The order of bond distances to the Ni1 center is Ni1—O1 < Ni1—N3 < Ni1—N1 < Ni1—P1, and these distances are comparable with those reported for other nickel(II) complexes having an O,N,N tridentate thiosemicarbazone and a triphenylphosphine as ligands[30,51,52]. As can be seen from the *cis* and *trans* angles in Table 2, the Ni^{II} ion has a distorted square-planar environment.

Table 2.

Experimental and Optimized Geometrical Parameters of the Title Compound

Parameters	Experimental	Calculated
Bond lengths (Å)		
Ni1—P1	2.2292(7)	2.2804
Ni1—O1	1.8272(18)	1.8384
Ni1—N1	1.867(2)	1.8806
Ni1—N3	1.864(2)	1.8785
Br1—C6	1.904(3)	1.9186
S1—C1	1.782(4)	1.8320
S1—C2	1.744(3)	1.7703
O1—C9	1.315(3)	1.3092
N1—C2	1.302(3)	1.3185
N2—C2	1.333(3)	1.3344
N2—N3	1.393(3)	1.3870
N3—C3	1.294(3)	1.3019
Bond angles (°)		
O1—Ni1—N3	93.46(8)	93.8369
O1—Ni1—N1	174.07(9)	176.3664
N3—Ni1—N1	82.44(9)	82.5382
O1—Ni1—P1	90.02(6)	88.8247
N3—Ni1—P1	173.70(7)	177.3306
N1—Ni1—P1	94.46(7)	94.8012
C2—S1—C1	103.16(14)	104.5154
C2—N2—N3	112.6(2)	112.4968
C3—N3—N2	117.2(2)	117.7887
N1—C2—N2	116.9(2)	117.6404
N1—C2—S1	122.2(2)	120.7150
N2—C2—S1	120.9(2)	121.6431
N3—C3—C4	122.0(2)	122.9362

In the crystal structure, the cationic complex is connected to the anion *via* N2—H2···C11 and C3—H3···C11 hydrogen bonds forming an $R_2^1(6)$ ring[53]. Besides, isothioamide nitrogen atom N1 and triphenylphosphine carbon atom C17 act as hydrogen-bond donor to isopropyl oxygen atom O2, so forming together an$R_2^1(8)$ ring (Fig. 2). The molecules translated linearly along $[1\bar{1}0]$ direction are linked to each other by means of C—H···Br interactions forming a molecular chain. Finally, inversion-related molecular chains are connected to each other by one O—H···Cl and one π—π stacking interactions. In these interactions, isopropyl oxygen atom O2 in the molecule at (*x*, *y*, *z*) acts as hydrogen-bond donor to the Cl^- anion in the molecule at (–*x* + 1, –*y* + 1, –*z* + 1), while the C4-C9 benzene ring in the molecule at

(*x*, *y*, *z*) stacks above the ring at (–*x*, –*y* + 2, –*z* + 1) with a distance of 3.7103(18) Å between the ring centroids. Full details of the hydrogen-bonding interaction are given in Table 3.

Table 3.

Hydrogen Bonding Geometry for the Title Compound

D—H···A	D—H (Å)	H···A (Å)	D···A (Å)	D—H···A (°)
O2—H2O···Cl1[i]	0.82	2.38	3.168(3)	161
C1—H1A···Br1[ii]	0.96	2.84	3.749(3)	158
C17—H17···O2	0.93	2.45	3.301(5)	153
N2—H2···Cl1	0.86	2.33	3.100(3)	150
N1—H1···O2	0.86	2.26	3.025(3)	148
C3—H3···Cl1	0.93	2.63	3.417(3)	143

[i] –*x* + 1, –*y* + 1, –*z* + 1; [ii] *x*+ 1, *y* − 1, *z*.

The molecular structure of the title compound was studied theoretically, and the calculated geometrical parameters are also given in Table 2. As can be seen from the table, the agreement between the experimental and theoretical structures is quite satisfactory.

Bond distances agree within 0.05 Å, while the largest deviation of bond angles appears to be 3.63°. Theoretically, the dihedral angle between the thiosemicarbazone ligand and coordination plane has been calculated at 2.622°. Although the experimental structure belongs to solid phase and theoretical structure belongs to gaseous phase, the calculated values adequately describe the experimental geometry and can be used to compute the other parameters.

Subsequent attempts to find the global energy minimum structure of the azine form of the title complex by theoretical calculations were not successful, and this confirms that the azinylidene form is stable than the azine form.

3.2. Atomic charge and molecular electrostatic potential. The NPA (Natural Population Analysis) atomic charge distributions on the atoms of the title complex and singly deprotonated thiosemicarbazone ion were calculated by applying the same method and the basis sets as used for geometry optimization. According to the calculated NPA atomic charges, the transferred electronic number from the thiosemicarbazone ion to central Ni(II) ion to form the title complex is found to be –0.90349 e.

Fig. 3 shows the molecular electrostatic potential (MEP) plot of the compound. Potential increases in the order red < orange < yellow < green < blue. The color code of the map is in the range between –0.082 a.u. (deepest red) and 0.037 a.u. (deepest blue) in the compound, where blue indicates the strongest attraction and red indicates the strongest repulsion. According to the MEP map, the minimum negative potential is localized on the chloride anion while the maximum positive region is localized on the H atom of the isopropyl oxygen atom. In addition, the electrostatic potentials on the bromine and isothioamide nitrogen H atoms are found to be –0.030 and 0.026 a.u. Consequently, Fig. 3 supports the existence of intermolecular interactions observed in the solid state.

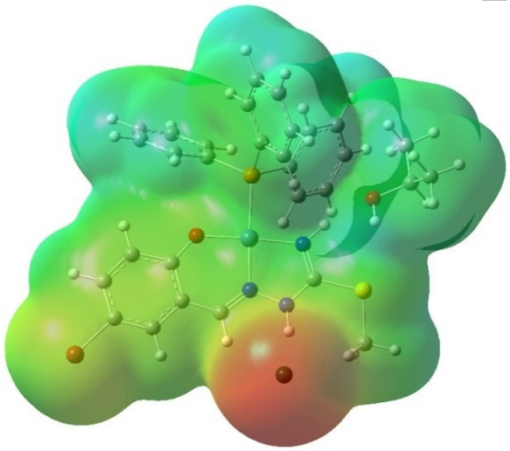

Fig. 3. Molecular electrostatic potential map of the title compound with an isodensity value of 0.0004 a.u.

3.3. IR spectra. The three bands at 3476, 3276 and 1632 cm^{-1} corresponding to asymmetric stretching, symmetric stretching and in-plane bending modes of (N^4—H_2), respectively, for the ligand were absent in the IR spectra of the complex. These bands have been calculated at 3641, 3524 and 1607 cm^{-1}, respectively. A medium intensity band appeared at 3084 cm^{-1} corresponding to phenolic *ν*(O—H) vibration in the ligand, which was determined theoretically at 3220 cm^{-1}, disappeared in the spectra of the complex indicating deprotonation. These are strong evidences that the ligand is coordinated to the metal ion *via* the amine nitrogen and phenolic oxygen atoms. A band that observed at 1153 cm^{-1} due to phenolic *ν*(C—O) stretching in the free ligand has been shifted to higher frequency by 25 cm^{-1} in the complex further corroborating the coordination through the phenolic oxygen atom. These bands were appeared at 1280 and 1306 cm^{-1} in the theoretical spectra of the ligand and complex, respectively. The IR spectra of the uncomplexed thiosemicarbazone ligand showed strong absorptions at 1627 and 1607 cm^{-1} due to the azomethine *ν*(C=N) groups, which were calculated at 1629 and 1608 cm^{-1},

respectively. These absorptions at the complex have been shifted to lower frequencies at 1562 and 1520 cm^{-1} that have been calculated at 1608 and 1522 cm^{-1}, respectively, in the complex indicating the coordination of the azomethine nitrogen to nickel ion.

In the complex spectra, stretching frequency of N—H was monitored at 3265 cm^{-1} as the broad band, and the other band assigned to *ν*(N—H) was at 2650 cm^{-1} because of the hydrogen bonding association between N^2—H and Cl[54].The IR bands at 2965, 2920, 2814 cm^{-1} corresponding to *ν*(C—H) vibrations are characteristic for isopropyl alcohol. However the stretching frequency of isopropyl alcohol O—H could not be clearly observed due to the expanded band of N—H stretching vibrations and the intermolecular hydrogen bonding.

3.4. ^{1}H-NMR spectra. The formation of the complex was also confirmed by its ^{1}H-NMR spectrum. The most remarkable peaks are to which was assigned to N^2H and N^4H. The hydrazinic N^2–H proton were observed downfield (at 11.61 and 10.75 ppm) because of acidic character and intramolecular interaction, while N^4H proton were observed upfield (at 7.91 and 6.99 ppm). These signals have been obtained at 11.35 and 4.69 ppm theoretically. In addition, C-H signal of imine group on the ligand was observed at 8.41 and 8.30 ppm in the complex due to intermolecular interaction that has been calculated at 10.02 ppm. All of these signals were appeared with line broadening. The broadening is because of the formed hydrogen bonds between N^2H and Cl atom, and between N^4H and isopropyl alcohol (Fig. 2).

Consequently, the ^{1}H-NMR chemical shifts of the thiosemicarbazone ligand and complex are in agreement with the direct bonding through $O_{hydroxyl}$, N_{imine}, N_{amine} groups of the ligand with the metal center.

3.5. Electronic absorption spectra. The UV-vis spectra of the ligand and complex were shown in Fig. 4. The UV-Vis. spectrum of the ligand shows bands at 241, 298, 309, 342 and 356 nm attributed to π→ π* and n→ π* transitions corresponding to aromatic ring and phenol, the latter to azomethine and thioamide groups. The absorption spectrum of the complex exhibits the bands at 239, 263, 355, 386, 406 and 529 nm attributed to π→ π* and n→ π*, Sorent band (B band), charge transfer and d-d transitions. By comparing these two spectra, the absorbance at 239 nm increases on complexation of PPh_3, and the shifts of the bands approve that thiosemicarbazone coordinates to nickel center by hydroxyl and amine moieties and are consistent with square-planar geometry of the complex[55-57].

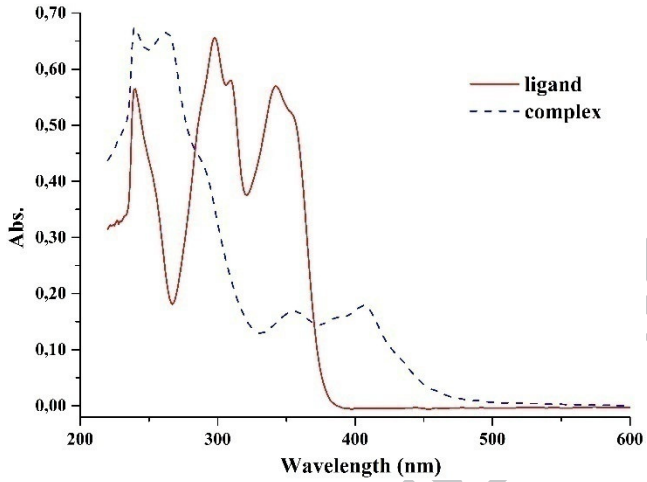

Fig. 4.UV-Vis. spectra of the ligand and complex.

Electronic absorption spectra of the ligand and complex were calculated by the TD-DFT method using the same basis set. The major contributions of the transitions were designated with the aid of GaussSum program[58].The most important orbitals in a molecule are the frontier molecular orbitals, called highest occupied molecular orbital (HOMO; H hereafter) and lowest unoccupied molecular orbital (LUMO; L hereafter). The frontier molecular orbitals play an important role in the electric and optical properties, as well as in UV-Vis. spectra and chemical reactions[59].

The frontier molecular orbitals of the ligand and complex are given in Fig. 5 and 6, respectively.

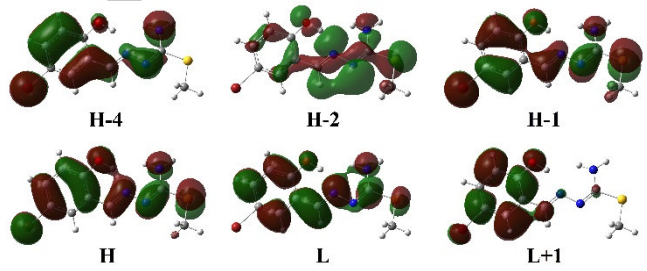

Fig. 5. Molecular orbital surfaces of the ligand. The positive phase is red, and the negative phase is green.

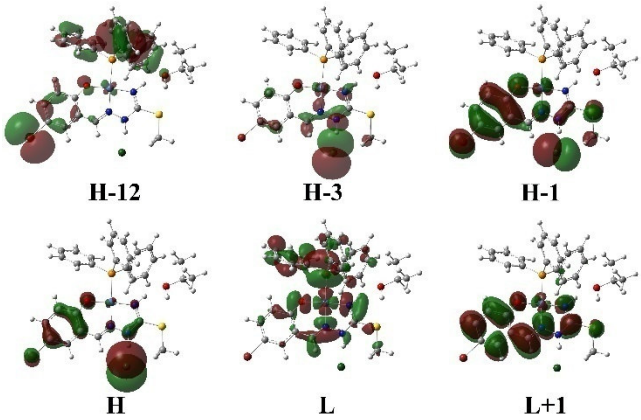

Fig. 6. Molecular orbital surfaces of the complex. The positive phase is red, and the negative phase is green.

TD-DFT calculations predict absorptions at 227 nm [major contributions: H–4→L (70%) and H–1→L+1 (12%)], 249 nm [major contributions: H→L+1 (75%) and H–4→L (13%)], 298 nm [major contributions: H–1→L (71%) and H–2→L (19%)] and 344 nm [major contribution: H→L (96%)] for the ligand, and at 326 nm [major contributions: H–1→L+1 (50%) and H–1→L (32%)], 380 nm [major contribution: H→L+1 (82%)], 389 nm [major contribution: H→L (63%)], 500 nm [major contributions: H–1→L (18%) and H–12→L (16%)], 574 nm [major contributions: H–3→L (50%) and H–3→L+1 (26%)] and 617 nm [major contributions: H→L (21%), H–1→L (18%)] and H→L+1 (10%)] for the complex. In addition, the value of the energy separation between the H and L is 4.058 eV for the ligand and 3.519 eV for the complex, indicating the stable nature of the compounds.

3.6. Thermal analysis. Fig. 7 shows the thermal (in nitrogen atmosphere) and thermal-oxidative decomposition (in air atmosphere) of the complex. TGA and DTA curves of the complex were obtained in the nitrogen and air atmosphere, and the curves of the complex in both atmosphere were different from each other. The thermal decompositions of the thiosemicarbazone complexes have been studied by many researchers and show similar thermal decomposition behavior. The observed trend is the formation of NiO or NiS as final residue[60].However, the synthesized nickel complex in this study showed unexpected behavior.

In the first decomposition step in air atmosphere, there was a weight loss of 8.60% in the region 35-147°C. The first decomposition product was isopropyl alcohol and this step was endothermic. The first decomposition step is different in nitrogen atmosphere than in air atmosphere. There was a weight loss of 6.70 % assigned to S—CH_3 part in the region 121-150°C[61].

It was observed unusual state in air atmosphere. We expected the formation of metal oxides as final residue. However, volatilization of nickel took place in air atm[31,32,60,62]. The mass of the remaining product equals only 4.49% of the complex mass at the 986°C. This step was endothermic and completely different in the nitrogen atmosphere. The complex was thermally more stable with 22.76% remaining after 985°C in nitrogen atmosphere than in air atmosphere.

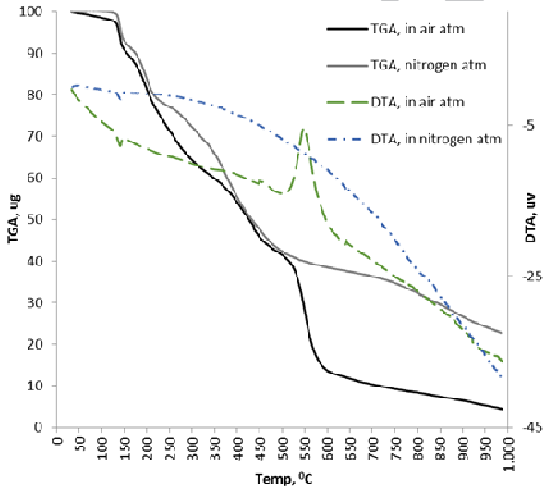

Fig. 7.TGA and DTA curves of the complex [TGA curves (dark solid line: in air atm., light solid line: in nitrogen atm.); DTA curves (long dash: in air atm., dash dot: in nitrogen atm.)].

3.7. Transfer hydrogenation of imine. The conversion of imine to amine is an important reaction in industrial applications, pharmaceutical processes and organic synthesis[63]. In this hydrogenation reactions, the catalysts have been used, such as 5% Pt–C, as a colloidal palladium (Skita), 10% Pd/C, platinum catalyst and a lot of transition metal complexes[64-68]. Isopropyl alcohol have been also used as hydrogen source in the reduction of imines to amines in the presence of metal complexes[69-72].

Unlike those of other studies, this paper presents that isopropyl alcohol catalyzes efficiently the transfer hydrogenation in solvent having appropriate polarity.

After our investigation results, we saw that there are fewer researches on tautomerizations of azinyl structures[73-77].It is known that an increase in the solvent polarity on azinyl⇄ azinylidene equilibrium leads to favor of ylidene tautomer[71,75,78,79].

We know that crystalline neutral complex was mainly in azine form in our previous study[30]. However, in this study, ionic tautomerization occured by orientation of the double bond in azine structure in mixture of ethanol, isopropyl alcohol and dichloromethane(v/v/v:1/3/1) in contrast to mixture of ethanol and dichloromethane, and azinylidene structure is formed by intramolecular proton transfer. This situation is unusual and unexpected for thiosemicarbazone complex. We imagined the following possible mechanism (Scheme 3).

In the reaction between thiosemicarbazone ligand and $[Ni(PPh_3)_2Cl_2]$, nickel bearing triphenylphosphine groups and a chlorine atom is connected to hydroxyl group of thiosemicarbazone ligand, while one HCl molecule removes from the reaction media (Scheme 3). However, large chlorine atom and bulky triphenylphosphine groups cause to steric effect around nickel atom and this case brings about unstable structure. As a result of instability, a rearrangement occurs in the structure. The system will try to create the most stable structure with minimum energy. This situation is provided the following ways: the chlorine atom and hydrogen atom of N^4_{amide} leaves as hydrogen chloride especially on treatment with isopropyl alcohol, later forms thioamide ion (this was shown with resonance in scheme 3, yellow field) and coordinates to nickel center. Meanwhile, one of bulky triphenylphosphine molecules left from the structure, too. (Scheme 3)

Scheme 3. The Proposed Reaction Mechanism of the Complex **I** Formation

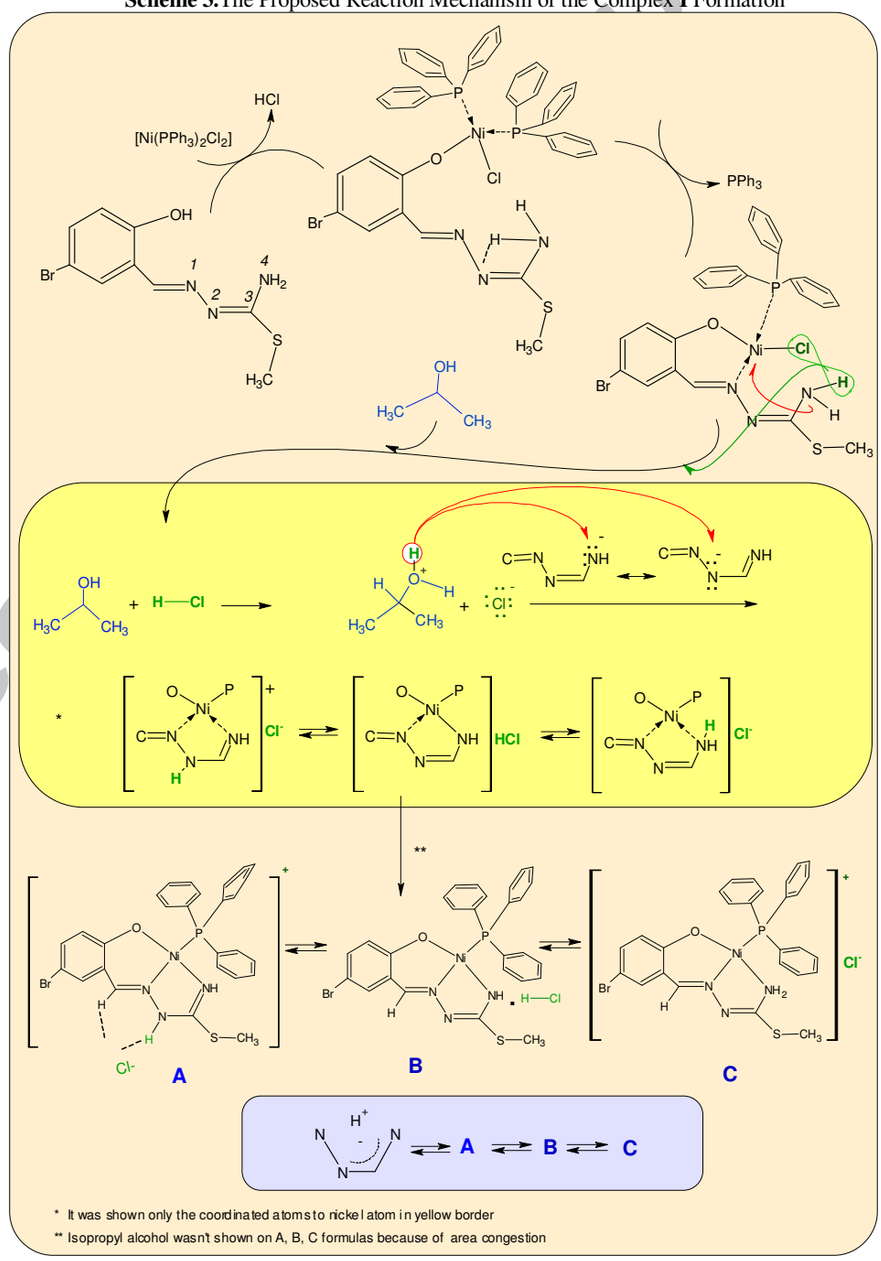

The reaction of isopropyl alcohol with the released hydrogen chloride acid, the lone pairs on the oxygen of the alcohol make it a Lewis base and allocates the proton from acid and forms chloride anion with oxonium cation (Scheme 3, yellow field). The oxonium ion supplies hydrogen for thioamide ion. So, isopropyl alcohol behaves as hydrogen transporter. This rearrangement is characterized by a 1,3-shift of an hydrogen atom from the N^4 atom to the N^2 atom site either in a stepwise mechanism or in a concerted one as depicted in Scheme 3. Electrophilic reagents such as Lewis acids can also promote this kind of rearrangement. The azinyl⇄ azinylidene equilibrium leads to favor of ylidene tautomer. The stable structure A through A ⇄ B ⇄ C transformations is obtained [73,75-77].

The results obtained experimentally and proposed mechanism were in good agreement with DFT values. The energy difference between structures A and C is found as 5.23 kcal mol^{-1} while structure B is not obtained due to the relative instability. Structure A is considerably stabilized by intermolecular hydrogen bonding between N^2H atom of the cationic complex and chloride anion, and is the most stable one according to the DFT calculations.

4. Conclusions

As a result, the reaction of S-methyl-isothiosemicarbazone compound and $[Ni(PPh_3)_2Cl_2]$ gave chloride salt of cationic thiosemicarbazone complex, $[Ni(LH)PPh_3]^+Cl^-\cdot(CH_3)_2CHOH$. The cationic form was successfully formed *via* hydrogen transfer. Isopropyl alcohol catalyzed efficiently the transfer hydrogenation by providing appropriate polarity media and the compound (**I**) formed through interconversion azinyl-azinylidene. The spectral data and x-ray analysis proved that azinylidene structure was stabilized by intramolecular proton transfer and by intermolecular interactions and hydrogen bondings.

X-ray analysis reveals that the thiosemicarbazone ligand coordinated to nickel as a tridentate monobasic chelator *via* O,N,N atoms. The crystalline lattice involves a chloride ion and an isopropyl alcohol molecule, also. The isopropyl alcohol has two acceptors (electron pairs of O atom) and only one donor (H atom), and give three hydrogen bonds. That is, H atom of the alcoholic hydroxyl group forms a hydrogen bond with Cl atom of the other molecule, and O atom of hydroxyl group forms two hydrogen bonds with hydrogen atoms of N1-H of thiosemicarbazone and of C17-H of PPh_3. Thus, the hydrogen bridges between protons of isopropyl alcohol, thiosemicarbazone and triphenylphosphine, and six-membered ring between chlorine atom and hydrogen atoms of N2-H and C3-H of thiosemicarbazone complex provide extra stability in formed solute-solvent complex structure. So, the structure is fixed by the hydrogen bonds. This framework is prepared from molecules "self-associate" via multiple hydrogen-bonding interactions.

The DFT calculations show that structure A is more stable than the other tautomers.

The decomposition of the compound was investigated by using thermogravimetry. The synthesized nickel complex showed unexpected behavior. The oxidative thermal decomposition shows volatilizing nickel complex of thiosemicarbazone nature as unusual.

Appendix A. Supplementary data

CCDC 1044168 contains the supplementary crystallographic data for the compound reported in this article. These data can be obtained free of charge via http://www.ccdc.cam.ac.uk/conts/retrieving.html, or from the Cambridge Crystallographic Data Centre, 12 Union Road, Cambridge CB2 1EZ, UK; fax: (+44) 1223-336-033; or e-mail: deposit@ccdc.cam.ac.uk.

Acknowledgement

This work was supported by the Research Fund of Istanbul University.

References

[1] B.Atasever, B.Ülküseven, T. Bal-Demirci, S.Erdem-Kuruca, Z. Solakoğlu, Invest. New Drugs28 (2010) 421-432.
[2] T. Bal, B.Atasever, Z.Solakoğlu, S.Erdem-Kuruca, B. Ulkuseven, Eur. J. Med. Chem. 42 (2007) 161-167.
[3] M.C. Rodriguez-Arguelles, E. Lopez-Silva, J.Sanmartin, P.Pelagatti, F. Zani, J. Inorg. Biochem. 99 (2005) 2231-2239.
[4] N.S. Moorthy, N.M. Cerqueira, M.J. Ramos, P.A. Fernandes, Recent Pat Anticancer Drug Discov. 8 (2013) 168-182.
[5] T. Bal-Demirci, M.Şahin, M.Özyürek, E.Kondakçı, B. Ulkuseven, Spectrochim. Acta Part A. 126 (2014) 317-323.
[6] R.C. DeConti, B.R. Toftness, K.C. Agrawal, R.Tomchick, J.A. Mead, J.R.Bertino, A.C. Sartorelli, W.A. Creasey, Cancer Res. 32 (1972) 1455-1462.
[7] D.R. Richardson, P.C. Sharpe, D.B. Lovejoy, D.Senaratne, D.S.Kalinowski, M. Islam, P.V. Bernhardt, J Med Chem. 49 (2006) 6510-6521.
[8] H. A. Zamani, Anal. Lett. 41 (2008) 1850-1866.
[9] N. Nuriman, B. Kuswandi, and W. Verboom, Sens. Actuators B 157 (2011) 438-443.
[10] K.H. Reddy, N.B.L. Prasad, T.S. Reddy, Talanta, 59 (2003) 425-433.
[11] F. Salinas, J.C. Jimenez Sanchez, T. Galeano Diaz, Anal. Chem.58 (1986) 824-827.
[12] J.S. Casas, M.S. Garcia-Tasende, J. Sordo, Coord. Chem. Rev. 209 (2000) 197-261.
[13] Ş.Güveli, A.Koca, N.Özdemir, T. Bal-Demirci, B. Ülküseven, New J. Chem.38(2014) 5582-5589.
[14] R. Yanardag, T. Bal Demirci, B. Ülküseven, S.Bolkent, S.Tunali, Ş. Bolkent, Eur. J. Med. Chem. 44 (2009) 818-826.
[15] N Özdemir, M Şahin, T Bal-Demirci, B Ülküseven, Polyhedron 30 (3), (2011) 515-521
[16] T. Bal, B. Ülküseven, Transit. Metal Chem. 29 (2004) 880-884.
[17] T.S.Lobana, P.Kumari, R.J. Butcher, J.P. Jasinski, J.A. Golen, Z Anorg. Allg. Chem. 638(2012) 1861-1867.
[18] P.K. Panchal, P.B.Pansuriya, M.N. Patel, J Enzym. Inhıb Med Ch. 21 (2006) 453-458.
[19] D.X. West, M.M.Salberg, G.A. Bain, A.E. Liberta, Transit. Metal Chem. 22 (1997) 180-184.
[20] T. Demirci, Y. Köseoğlu, S. Güner, B. Ülküseven, *Cent. Eur. J Chem* (*Open Chem.*). 4 (1), (2006) 149–159, DOI: 10.1007/s11532-005-0011-z
[21] T. Bal-Demirci, M.Akkurt, Ş.P.Yalçın, O. Büyükgüngör, Transit. Metal Chem. 35 (2010) 95-102.
[22] A.E.Liberta, D.X. West, BioMetals 5 (1992) 121-126.
[23] A.Basu, G. Das, Dalton Trans. 40(2011) 2837-2843.
[24] T. Bal-Demirci, Polyhedron 27 (2008) 440-446.
[25] I. Pal, F.Basuli, S. Bhattacharya, J. Chem. Sci. 114 (2002) 255-268.
[26] N. J. Turro, *PNAS,* 102(31)(2005) 10766-10770
[27] R. Alonso, E. Bermejo, R. Carballo, A.Castiñeiras, T. Pérez, J. Mol. Struct. 606 (2002) 155-173.
[28] A.Castiñeiras, N.Fernández-Hermida, R.Fernández-Rodríguez, I. García-Santos, Cryst. Growth Des. 12 (2012) 1432-1442.
[29] Yu.A. Simonov, M.D.Revenco,P.N.Bourosh, P.I.Bulmaga, M.Gdaniec, Crystallogr. Reports 54 (2009) 893-897.
[30] Ş.Güveli, T. Bal-Demirci, N.Özdemir, B. Ülküseven, Transit. Metal Chem. 34 (2009) 383-388.
[31] T. Maruyama, and T.Tago, J. Mater. Sci.28 (1993) 5345-5348.
[32] V.V.Bakovets, V.N. Mitkin, and N.V. Gelfond, Chem. Vapor. Depos. 11 (2005) 112-117.
[33] B.Ulkuseven, T. Bal-Demirci, M.Akkurt, Ş.P.Yalcın, O. Buyukgungor, Polyhedron 27 (2008) 3646-3652.
[34] Stoe&Cie, X-AREA Version 1.18 and X-RED32 Version 1.04, Stoe&Cie, Darmstadt, Germany, (2002).
[35] G.M. Sheldrick,Acta Crystallogr. C71 (2015) 3-8.
[36] L.J.Farrugia, J. Appl. Crystallogr. 45 (2012) 849-854.
[37] A.D.Becke, J. Chem. Phys. 98 (1993) 5648-5652.
[38] C.Lee, W. Yang, R.G. Parr, Phys. Rev. B37 (1988) 785-789.
[39] P.J. Hay, W.R.Wadt, J. Chem. Phys. 82 (1985) 270-283.
[40] P.J. Hay, W.R.Wadt, J. Chem. Phys. 82 (1985) 284-298.
[41] P.J. Hay, W.R.Wadt, J. Chem. Phys. 82 (1985) 299-310.
[42] A.D. McLean, G.S. Chandler, J. Chem. Phys. 72(1980) 5639-5648.
[43] K.Raghavachari, J.S. Binkley, R. Seeger, J.A. Pople, J. Chem. Phys. 72 (1980) 650-654.
[44] R. Ditchfield, J. Chem. Phys. 56 (1972) 5688-5691.
[45] K.Wolinski, J.F. Hinton, P. Pulay, J. Am. Chem. Soc. 112 (1990) 8251-8260.
[46] R.I.I.Dennington, T. Keith, J. Millam, *Gauss View, Version 4.1.2,*Semichem Inc., Shawnee Mission, KS, 2007.
[47] M.J. Frisch, G.W. Trucks, H.B. Schlegel, G.E.Scuseria, M.A. Robb, J.R. Cheeseman, J.A. Montgomery Jr., T.Vreven, K.N.Kudin, J.C.Burant, J.M.Millam, S.S.Iyengar, J.Tomasi, V. Barone, B.Mennucci, M.Cossi, G.Scalmani, N.Rega, G.A.Petersson, H.Nakatsuji, M.Hada, M.Ehara, K. Toyota, R. Fukuda, J. Hasegawa, M. Ishida, T. Nakajima, Y. Honda, O. Kitao, H.Nakai, M.Klene, X. Li, J.E. Knox, H.P.Hratchian, J.B. Cross, V. Bakken, C.Adamo, J. Jaramillo, R.Gomperts, R.E.Stratmann, O.Yazyev, A.J. Austin, R.Cammi, C.Pomelli, J.W.Ochterski, P.Y.Ayala, K.Morokuma, G.A.Voth, P. Salvador, J.J. Dannenberg,V.G.Zakrzewski, S.Dapprich, A.D. Daniels, M.C. Strain, O.Farkas, D.K.Malick, A.D.Rabuck, K.Raghavachari, J.B.Foresman, J.V. Ortiz, Q. Cui, A.G.Baboul, S. Clifford, J.Cioslowski, B.B.Stefanov, G. Liu, A.Liashenko, P.Piskorz, I. Komaromi, R.L. Martin, D.J. Fox, T. Keith, M.A. Al-Laham, C.Y. Peng, A.Nanayakkara, M.Challacombe, P.M.W. Gill, B. Johnson, W. Chen, M.W. Wong, C. Gonzalez, J.A.Pople, Gaussian 03, Revision E.01, Gaussian, Inc., Wallingford CT, 2004.
[48] E.Cancès, B.Mennucci, J. Tomasi, J. Chem. Phys. 107 (1997) 3032-3041.
[49] R.E.Stratmann, G.E.Scuseria, R. Frisch, J. Chem. Phys. 109 (1998) 8218-8224.
[50] M.E.Casida, C.Jamorski, K.C.Casida, D.R. Salahub, J. Chem. Phys. 108 (1998) 4439-4449.
[51] Ş.Güveli, B.Ülküseven, Polyhedron 30 (2011) 1385-1388.
[52] P.Kalaivani, R.Prabhakaran, F.Dallemer, K.Natarajan, RSC Adv. 94 (2014) 51850-51864. https://dx.doi.org/10.1039/C4RA08492F

[53] J. Bernstein, R.E. Davis, L.Shimoni, N.-L. Chang, Angew. Chem. Int. Ed. Engl. 34 (1995) 1555-1573.
[54] M.S.Refat, H.Al.Didamony, K.M. Abou El-Nour, L. El-Zayat, A.M.A. Adam, Arabian J. Chem. 4 (2011) 105-114. https://dx.doi.org/10.1016/j.arabjc.2010.06.026
[55] A.Famengo, D. Pinero, O.Jeannin, T.Guizouarn, M. Fourmigué, Dalton Trans. 41 (2012) 1441-1443.
[56] M.B. Ferrari, S.Capacchi, F.Bisceglie, G. Pelosi, P. Tarasconi, Inorg. Chim. Acta 312 (2001) 81-87.
[57] V.M.Leovac, L.S.Jovanović, V.Divjaković, A.Pevec, I. Leban, T. Armbruster, Polyhedron 26 (2007) 49-58.
[58] N.M. O'Boyle, A.L.Tenderholt, K.M. Langner, J. Comp. Chem. 29 (2008) 839-845.
[59] I. Fleming, Frontier Orbitals and Organic Chemical Reactions, John Wiley & Sons, Ltd, Chichester,, 1976.
[60] A. Manohar, K.Ramalingam, K. Karpagavel, Int.J. ChemTech Res. 6(5) (2014) 2620-2627.
[61] T. Bal, B. Ülküseven, Russ. J. Inorg. Chem. 49 (2004) 1685-1688.
[62] S.Arockiasamy, O.M.Sreetharan, C.Mallika, V.S.Raghunathan, K.S. Nagaraja, Chem. Eng. Sci. 62 (2007) 1703-1711.
[63] G.C.K. Roberts, Drug Action at the Molecular Level, University Park Press, Baltimore, 1977.
[64] M. Freifelder, Catalytic Hydrogenation in Organic Synthesis. Procedures and Commentary; John Wiley, New York, 1978, pp.56-69.
[65] M.L.Heyman, J.P. Snyder, Tetrahedron Lett. 14 (1973) 2859-2862.
[66] K.A. Taipale, Ber. Dtsch. Chem. Ges. 56 (1923) 954-962.
[67] J.Easmon, , G. Heinisch, G.Pürstinger, T. Langer, J.K.Österreicher, H.H.Grunicke, J. Hofmann, J. Med. Chem. 40 (1997) 4420-4425.
[68] H.H. Fox, J.Y. Gibas, J. Org. Chem. 20 (1955) 60-69.
[69] F.A. Carey, Organic Chemistry, Chapter 4, 4th Edition, McGraw Hill, 2000.
[70] J.S.M.Samec, L.Mony, Jan-E. Bäckvall, Can. J. Chem. 83 (2005) 909-916.
[71] C. Masters, B.L. Shaw, R.E. Stainbank, J. Chem. Soc. D., Chem. Commun. (1971) 209-209.
[72] S.lyer, J.P. Varghese, J. Chem. Soc., Chem. Commun. 4 (1995) 465-466.
[73] S.A.Stekhova, O.A.Zagulyaeva, V.V.Lapachev, V.P. Mamaeva, Chem. Heterocycl. Compd. 16 (1980) 640-644.
[74] O.P.Petrenko, V.V.Lapachev, I.K.Korobeinicheva, V.P. Mamaev, Chem. Heterocycl. Compd. 23 (1987) 1343-1347.
[75] S.Moulay, Chem. Educ. Res. Pract. 3 (2002) 33-64.
[76] V.V.Lapachev, O.P.Petrenko, V.P.Mamaev, Russ. Chem. Rev. 59 (1990) 457-482.
[77] I. Ya.Mainagashev, O.P.Petrenko, V.V.Lapachev, M.A. Fedotov, I.K.Korobeinicheva, V.P. Mamaev, Chem. Heterocycl. Comp, 24 (1988) 424-430.
[78] O.A.Zagulyaeva, I.V. Oleinik, Chem. Heterocycl. Comp. 31 (1995) 715-725.
[79] T.Ohwada, N.Tani, Y.Sakamaki, Y.Kabasawa, Y.Otani, M. Kawahata, K. Yamaguchi, PNAS 110 (2013) 4206-4211.

Graphical abstract

Pictogram:

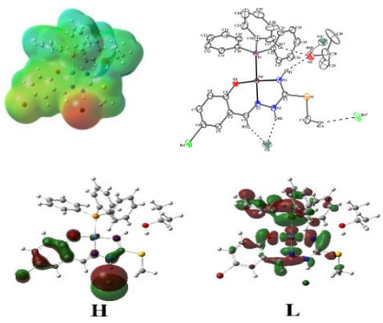

Graphical abstract

Synopsis:

The large energy gap of 3.519 eV between the HOMO (H) and the LUMO (L) indicates that the complex,$[Ni(LH)(PPh_3)]^+Cl^-.(CH_3)_2CHOH$, is very stable. This paper presents that isopropylalcohol catalyzes efficiently the transfer hydrogenation and a supramolecular structure forms. The oxidative thermal decomposition shows volatilizing nickel complex.